Global Change Biology

Global Change Biology (2010), doi: 10.1111/j.1365-2486.2010.02221.x

TECHNICAL ADVANCES

A method for experimental heating of intact soil profiles for application to climate change experiments

PAUL J. HANSON*, KENNETH W. CHILDS†, STAN D. WULLSCHLEGER*, JEFFERY S. RIGGS‡, WARREN K. THOMAS§, DONALD E. TODD* and JEFFREY M. WARREN*

*Environmental Sciences Division, Oak Ridge National Laboratory, Oak Ridge, TN 37831-6422, USA, †Computational Sciences & Engineering Division, Oak Ridge National Laboratory, Oak Ridge, TN 37831-6085, USA, ‡Campus Support and Instrumentation Division, Oak Ridge National Laboratory, Oak Ridge, TN 37831-6035, USA, §Facilities Development Division, Oak Ridge National Laboratory, Oak Ridge, TN 37831-6336, USA

Abstract

A new system for simulating future belowground temperature increases was conceived, simulated, constructed and tested in a temperate deciduous forest in Oak Ridge, TN, USA. The new system uses low-wattage, 3 m deep heaters installed around the circumference of a defined soil volume. The heaters add the necessary energy to achieve a set soil temperature differential within the treatment area and add exterior energy inputs equal to those, which might be lost from lateral heat conduction. The method, which was designed to work in conjunction with aboveground heated chambers, requires only two control sensor positions one for aboveground air temperatures at 1 m and another for belowground temperatures at 0.8 m. The method is capable of achieving temperature differentials of at least $+4.0 \pm 0.5\,^{\circ}C$ for soils to a measured depth of -2 m. These $+4\,^{\circ}C$ differential soil temperatures were sustained *in situ* throughout 2009, and both diurnal and seasonal cycles at all soil depths were retained using this simple heating approach. Measured mean energy inputs required to sustain the target heating level of $+4\,^{\circ}C$ over the 7.1 m^2 target area were substantial for aboveground heating (21.1 kW h day^{-1} m^{-2}), but 16 times lower for belowground heaters (1.3 kW h day^{-1} m^{-2}). Observations of soil CO_2 efflux from the surface of the target soil volumes showed CO_2 losses throughout 2009 that were elevated above the temperature response curve that have been reported in previous near-surface soil warming studies. Stimulation of biological activity within previously undisturbed deep-soil carbon stocks is the hypothesized source. Long-term research programs may be able to apply this new heating method that captures expected future warming and temperature dynamics throughout the soil profile to address uncertainties in process-level responses of microbial, plant and animal communities in whole, intact ecosystems.

Keywords: climate change, CO_2 efflux, drying, soil, warming

Received 16 February 2010 and accepted 23 February 2010

Introduction

With the release of the Fourth Assessment Report from the Intergovernmental Panel on Climate Change (IPCC, 2007), global climate change and its causes are now clearly established. In the absence of a change in human use of fossil fuels and global land management, atmospheric [CO_2] will continue to rise. As a result, global temperatures are projected to increase during the next century by as much as 5 °C, and precipitation amounts and patterns will change. A focus of future climate change research will be on consequences, and a critical component of new research will be the impacts of climate change on terrestrial ecosystems. Long-term monitoring of ecosystem responses is an important activity of the planned National Ecological Observatory Network (NEON), but such observations, by themselves, are insufficient to distinguish future climate change impacts from inherent developmental changes or responses to natural variability. A more powerful and integrative approach is to link site monitoring with manipulative ecosystem experiments to inform models and provide a basis for interpretation of data from monitored sites (Janzen, 2009).

Consensus Global Circulation Model (GCM) projections of the climatic and atmospheric changes from the IPCC Fourth Assessment Report suggest a mean warming of 3.8 and 3.3 °C during the winter and summer, respectively, by the end of this century for the IPCC A1B greenhouse gas emission scenarios (Christensen *et al.*, 2007). Projected extreme summer

Correspondence: P. J. Hanson, tel. +1 865 574 5361, fax +1 865 576 9939, e-mail: hansonpj@ornl.gov

Published 2010
This article is a US Government work and is in the public domain in the USA

heat events may also expose ecosystems to acute stress that exceeds historical and contemporary long-term conditions to which extant vegetation is adapted. Based on current greenhouse gas production (Raupach *et al.*, 2007), forcing estimates even greater than those applied in the A1B scenario (Christensen *et al.*, 2007) are now likely. Therefore, even greater levels of warming need to be considered as drivers for ecological responses and impacts evaluations. Such levels of warming exceed the observed variation in mean annual temperatures ($\pm 2\,^{\circ}$C) and atmospheric conditions under today's climate and represent a range of conditions that necessitate experimental manipulation (Hanson *et al.*, 2008).

Designing and constructing experiments capable of directly testing biological responses is a necessary prerequisite for the evaluation of model projections. Experiments have been accomplished to study impacts of warming on terrestrial ecosystems (e.g., Rustad & Fernandez, 1998; Shaver *et al.*, 2000; Rustad *et al.*, 2001; Kimball, 2005; Dermody *et al.*, 2007; Bronson *et al.*, 2008), but advances in mechanistic understanding would benefit from new and more realistic approaches to exposing ecosystems and their component organisms to increased temperatures (Tjoelker & Zhou, 2007). This need exists across a range of spatial scales, from small open-top chambers to larger designs culminating in the operation of *in situ* studies in field research settings. Past and ongoing heating methods focused on the elevation of air temperatures (Norby *et al.*, 1997; Medhurst *et al.*, 2006), surface temperatures (Nijs *et al.*, 1996; Kimball, 2005), near-surface soil temperatures (Peterjohn *et al.*, 1993; Melillo *et al.*, 2002) or both (Bronson *et al.*, 2008, 2009) to approximate the warming of ecosystems for studies of biological response.

Temperatures observed in biologically active surface soils (0 to -1 m or greater depths relevant to deep rooting and carbon storage) represent a dynamic balance between heat flows from surface air masses and stable deep soil temperatures (Huang, 2006; Hegerl *et al.*, 2007). Often overlooked in warming studies is the reality that deep soil temperatures will also become elevated as they equilibrate with new mean annual temperatures (Baxter, 1997; Hu & Feng, 2003). Such deep warming has not been achieved using previous warming technologies. Instead, preferential heating of surface soils has occurred as soils deeper in the profile remain unaffected. Previous warming studies have also not commonly reported warming below the surface soils, focusing instead on preferential warming of upper soils rich in organic carbon and intensive biologic activity. Although often characterized as a zone of lower carbon concentrations, deep soils contain significant carbon stocks and support quantifiable populations of roots and soil microbes that are unfortunately ignored in current warming studies.

To accommodate an experiment capable of providing deep warming conditions for experimental observations, a technology and protocol were developed for deep soil (-2 m) warming able to achieve belowground temperatures consistent with future aboveground warming scenarios. This paper describes the design, simulation, prototype construction and performance of facilities to study ecosystem response to climatic change conditions above- and belowground. To achieve realistic future warming conditions, ideal experimental systems should retain diurnal and seasonal temperature patterns of the target ecosystem throughout the soil profile. A deep, circumferential soil warming method described here, coupled with an open-top chamber modified for air temperature control (Norby *et al.*, 1997), meets this goal and avoids disturbance of root and microbial activity in the desired soil treatment volume. This paper describes the development and testing of such an experimental infrastructure and demonstrates its performance throughout an annual cycle for the understory of an upland oak forest in eastern Tennessee, USA. Observations of soil CO_2 efflux were conducted within the new prototype as one means of characterizing the utility and importance of deep soil warming.

Methods

Simulations of belowground heating options

Several belowground warming systems were conceptualized and modeled with the general-purpose heat conduction code HEATING 7.3 (Childs, 1993) to arrive at a suitable design for achieving acceptable patterns of temperature distributions throughout the soil–water matrix of the soil profile. Simulations were conducted for a soil volume that had a diameter of 3 m and a target soil depth of 1.5 m. Physical and thermal parameters used in the simulations are shown in Table 1. The original concept of a deep soil warming system was that of a defined soil volume accessed from an excavated trench (Fig. 1a). Such a system was plausible and a monolith version has previously been applied in controlled environments (e.g., the EcoCells; Verburg *et al.*, 2005). Deep-only soil warming proved impractical for *in situ* applications, however, because the deep horizontal heaters would have had to extend well beyond the edges of the target treatment soil volume, and were determined to require significant destructive excavations. The costs of excavations and the structural walls needed to safely support side access to the belowground soil depths were determined to be prohibitive. Infrared heating of the ground surface by itself was also simulated as an alternate design, but it did not achieve the desired temperature differential (ΔT) throughout the soil test volume (data not shown). The original concept was replaced by a novel deep-circumferential heating design (Fig. 1b).

The simulated deep-circumferential heating concept required the installation of a ring of vertically oriented exterior heaters just outside the perimeter of the defined soil volume to

Published 2010
This article is a US Government work and is in the public domain in the USA, *Global Change Biology*, doi: 10.1111/j.1365-2486.2010.02221.x

Table 1 Assumptions used to simulate the belowground energy status of a warmed soil volume

Climate data: Hourly air and humidity data for 2003 at 1 m; a year with average rainfall and temperatures for the Walker Branch forest

Air temperature at 1 m: + 4 °C over ambient air temperatures for Walker Branch

Soil volume characteristics: Uniform horizontal and vertical composition was assumed for simplicity. That is, we ignored [C], bulk density and textural changes with depth for these simulations

High soil moisture levels (the most energy demanding circumstance): Field capacity soil water content (v/v) at the surface (35%) declining to a constant 25% from −1 to −7 m

Soil thermal conductivity

Interpolated through the following values

Dry soil	0.2 W m-K^{-1}
7% moisture	1.0 W m-K^{-1}
13% moisture	1.25 W m-K^{-1}
50 % moisture	2.0 W m-K^{-1}

Soil volumetric heat capacity: 1. 1 MJ m^3-K^{-1} for dry soil increasing linearly to 3.15 MJ m^3-K^{-1} at 50% soil water content

Heat transfer coefficient between the air and the soil surface: 5 W m-K^{-1}

Solar heating: Direct solar heating of the soil surface was not considered in the simulations since the prototype was installed in an understory forest environment where such inputs were limited and comparable between heated and control plot areas (data not shown)

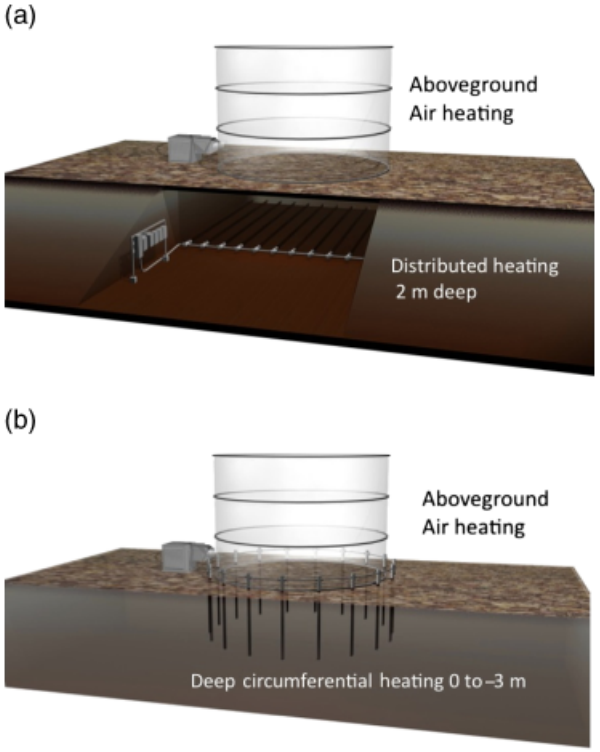

Fig. 1 Schematic diagrams of two approaches for imposing deep soil warming treatments within an *in situ* soil volume. While both can work, the bottom concept is easier to install and construct. (a) Original concept, (b) optimized alternative concept.

supply the energy for heating the target soil volume. Several variations of this design were examined through simulations. The number and spacing of the heaters was varied, the depth to which the heaters extended was varied, and the heater power and power distribution within the heater were varied. A design with 12 heaters that are 3 m long and equally spaced around a 3.5 m diameter circle simulated acceptable uniformity of ΔT within the test volume over 30 days. However, a design with 24 heaters gave better uniformity in ΔT and offered some redundancy in case of failure of some heating elements. Designs with separately controlled heating zones along the length of a single heater were also simulated. Although such an approach produced some improvement in the uniformity of ΔT within the test volume, the level of improvement did not justify the added complexity and cost. The final optimized design utilized uniform heating along the entire 3 m length of each heater.

Energy balance simulations were run to identify a design that controlled soil temperature throughout the target volume at a specified ΔT (+ 4 °C) above ambient soil temperatures. A secondary goal was to reach the desired ΔT within 30 days of the initiation of soil heating. Simulated temperature differentials for a 3 m plot diameter are shown in Fig. 2. The total belowground heater power in the simulation was 1.44 kW, but the heaters were operated at full power for only a brief period at the beginning of the initial heat-up transient. The heater power was then progressively reduced throughout the simulated 30-day period required to reach the desired steady operating conditions. Once steady conditions were reached the power input was a near-constant 0.216 kW. While limited temperature gradients were simulated within the target soil volume, the ± 0.5 °C range was considered acceptable performance.

Description of the constructed belowground warming prototype

To allow testing of the new warming approach, we combined existing aboveground forced-air heating technologies (Norby *et al*., 1997; Gunderson *et al*., 2010) to provide the requisite air warming for use with the new belowground heater arrangement. Aboveground heating was accomplished with open top chambers (3 m diameter) having single pass air flow rates of 0.78 m^3 s^{-1} passing across a an electrical resistance duct heater (220 V 7.5 kW; Farnam Custom Products, Arden, NC, USA). Evaporative cooling bats used in the Norby *et al*. (1997) configuration were not used for this work.

The heated systems along with a constructed control plot having identical structure, construction, disturbance and aboveground air velocities (Fig. 3) was deployed in the understory of an upland oak forest adjacent to the Walker Branch Watershed on the U.S. Department of Energy's (DOEs) National Environmental Research Park in Oak Ridge, Tennes-

Published 2010
This article is a US Government work and is in the public domain in the USA, *Global Change Biology*, doi: 10.1111/j.1365-2486.2010.02221.x

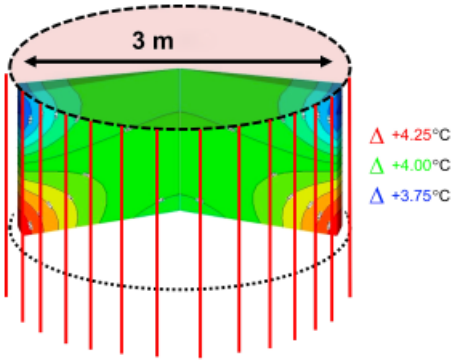

Fig. 2 Simulated steady-state temperature differentials to a depth of −1.5 m across the target soil volume of a 3 m diameter experimental plot. The simulation assumes an effective method for aboveground warming that would achieve air temperatures +4 °C over ambient conditions outside the chamber. Color gradients within the diagram cover only a 0.5 °C range, and correspond to the minimum, mid-point, and maximum shown at the right.

see (35°57.15′N latitude and 84°17.31′W longitude) Long-term climate, hydrology and soil data are available for this site (Johnson & VanHook, 1989; Hanson & Wullschleger, 2003). Long-term (50-year) mean annual precipitation is 1352 mm and mean annual temperature is 14.2 °C. The soils are primarily Typic Paleudults derived from dolomitic bedrock. Plant-extractable water (water held between 0 and −2.5 MPa) for the upper meter of soil at field capacity is approximately 183 mm.

Twenty-four belowground heaters were installed at an equally spaced interval around the circumference of a 3.5 m diameter circle just outside the walls of the open top chamber. Each individual 60 W 110 V U-bent heater (Part # 7121LB202408, Indeeco, St Louis, MO, USA) was installed from 0 to approximately −3 m within a length of 1 1/4 NPT Schedule 40 iron pipe with a sealed bottom (Fig. 3). The pipe was inserted into a drilled vertical hole in the soil backfilled with coarse sand. One heater within each quadrant was also instrumented with a thermocouple installed adjacent to the exterior of the iron pipe to serve as a high temperature cutoff. Temperature sensors installed at the surface of the iron pipes containing the heaters, as a high-temperature cutoff set for 40 °C, were typically only +4 to +5 °C higher than target soil temperatures within the plots, and were never measured higher than 27 °C throughout 2009. A shallow trench (10 cm wide by ∼20 cm deep) was also excavated just beyond the belowground heater pipes and filled with polyurethane foam to reduce horizontal surface heat conduction away from the treated area within the open top chamber.

The belowground heaters were wired in quadrant controls within the heated plots (six heaters per controller) to allow regulation of spatial differences within the heated plot. Thermocouples needed to control the belowground heaters were Type 'J' (W.H. Cooke Company, Hanover, PA, USA) and each was fitted with a 4–20 mA transmitter (Model minipaq-HLP, INOR Transmitter Inc., Peabody, MA, USA). The thermocouples within the heated plot were centered along a radius extending from the plot center to the chamber wall in each quadrant at a depth of 76 cm (30 in). Heated quadrant temperatures were controlled in reference to an identical thermocouple installed in the center of the control plot.

Fig. 3 Completed warming prototype and control chamber (upper picture with heated system on the left), a close-up photograph of the belowground heater connector head, and a diagram of a single belowground heater.

Although a full range of temperature differentials could be justified from global climate change predictions (Christensen *et al.*, 2007), to demonstrate the new deep soil heating method, a differential of +4 °C was chosen for evaluation throughout a full annual cycle. That differential is representative of projected global mean temperature increases for 2100 mid-latitude temperate regions. Controls and instantaneous displays of the belowground warming system were conducted with a proportional–integral–derivative controller (PID controller; Model 3504; Eurotherm, Leesburg, VA, USA) combined with SCR Power Controls (Model 18, Payne Engineering, Scott Depot, WV, USA). Air heating was controlled via the data logger program.

A capacity to humidify the air entering the heated chamber was added to the prototype in the summer of 2009 [day of the year (DOY) 222] to address the drying effect of heating technologies. Amthor *et al.* (2010) comment on the need for addressing humidity control in warming studies and, in the absence of specific direction from global climate models, suggest that conserving relative humidity with warming is a

This article is a US Government work and is in the public domain in the USA, *Global Change Biology*, doi: 10.1111/j.1365-2486.2010.02221.x

logical approach. A 220 V, 4600 W, single-phase electric-element steam humidifier capable of adding up to 6.22 kg h^{-1} of vaporized water to the air stream (Model UR006; Carel USA, Manheim, PA, USA) was installed to inject steam in the heated air flow entering the distribution plenum of the open top chamber (Norby *et al*., 1997).

Measures of performance

Temperatures. In addition to the control and heated-plot soil thermocouples described above, profiles of soil temperature by depth were also instrumented using vertically installed thermocouples (Model TMQSS: Type 'T' ungrounded thermocouples at custom lengths within 304 stainless steel sheaths, OMEGA Engineering Inc., Stamford, CT, USA) to evaluate the spatial performance of the method. Plot center and mid-radius profiles included the following eight depths: soil surface, −5, −10, −20, −40, −80, −160 and −200 cm. Four additional shallow profiles (−5, −20 and −40 cm) were installed to monitor potential gradients near the plot edges in the vicinity of the circumferential heaters. These shallow profiles were installed in line with selected heaters and at the mid-point between two heaters at 20 and 40 cm inwards from the circle of belowground heaters. Ambient air temperatures and two replicate deep soil temperature profiles were also recorded away from the manipulated plots, but within the understory of the forest stand.

Air temperature and relative humidity sensors (Model HMP-45C, Campbell Scientific Inc., Logan, UT, USA) were installed 1 m above the forest floor in the center of the heated and control plots to verify air heating levels and to quantify the humidity changes associated with the warming protocol. Soil-to-air vapor pressure deficit was calculated by contrasting the saturated surface soil vapor pressures (for measured surface soil temperatures) with the measured vapor pressure of well-mixed air within the open top chamber. Quantum sensors (Model Li190SA, LiCor Biosciences Inc., Lincoln, NE, USA) and litter wetness sensors (Hanson *et al*., 2003) were also installed within the heated and control plots to verify additional environmental variables important to the energy flow through the system.

Soil moisture. Four frequency domain reflectometry (FDR) soil moisture probes (Model CS616, Campbell Scientific Inc.) were installed in the heated and control plots. Two were installed vertically to obtain integrated soil moisture data from 0 to −30 cm, and two were installed at an angle to obtain integrated soil moisture data for the 0–15 cm depth. To obtain depth specific data at greater depths, frequency domain capacitance probes (Enviroscan, Sentek, Stepney, SA, Australia) were installed within and outside both plots at 20, 30, 40, 50, 60, 70 and 80 cm depths.

Energy use. Split core current transformers (Measurelogic Inc., Parker, CO, USA) were installed on one leg of the AC power circuits to evaluate the amperage of each device for energy use including: individual quadrants of belowground heaters (110 V ac), the aboveground air heater (220 V ac), aboveground air blowers (110 V ac) and the steam injection instrument (220 V ac). Each transformer is measured by an ac voltmeter (Model DP25-VRMS, OMEGA Engineering Inc.) using a multiplexer (Model AM 16-32, Campbell Scientific Inc.) to make the connection. An analog output from the ac voltmeter is measured and recorded by the data logger (Model CR10X, Campbell Scientific Inc.). The data logger was programmed to control and connect each current transformer to the ac voltmeter in turn and to record the mean hourly amperage. Amps were multiplied by the supply voltage to obtain watts of energy use.

Biological observations. To better understand the nature of soil organism responses to the new deep-soil warming method, various measures of biological response were conducted as replicate subsamples within the single prototype warming plot and its control (e.g., soil CO_2 efflux, [CO_2] by depth, ion exchange resin data by depth, microbial population assessments, root density changes). Here, we report on soil CO_2 emissions by depth. Soil CO_2 efflux at the forest floor was evaluated with an automated system including a CO_2 analyzer and control unit (LI-8100, LiCor Biosciences Inc.), a multiport sampling unit (LI-8150-8, LiCor Biosciences Inc.), and four automatic chambers designed to close periodically for the quantification of headspace CO_2 accumulation (LI-8100-104, Licor Biosciences Inc.). Two of the automated chambers were randomly positioned within the heated and the control chamber. Each chamber included a dedicated thermistor for soil temperature measurements LI-8150-203 installed at −10 cm, and a soil moisture probe (ECH2O EC-5 probes, Decagon Devices Inc., Pullman, WA, USA) installed from the surface to a depth of 10 cm. Each soil CO_2 efflux chamber and the associated temperature and moisture probes were evaluated every 15 min, with measurements in heated and control chambers alternating through time.

Results

Prototype operation and performance

Prototype heating was initiated January 7, 2009 (DOY 7; Fig. 4), and continued with only occasional power interruptions until November 13, 2009 (DOY 317). Belowground heaters continuously added 1.44 kW (24 circumferential heaters operating at 60 W) of energy initially, and achieved or overshot the target temperatures by DOY 18–22 depending on the soil depth (11–15 days, respectively). This initial rate of soil temperature increase was more rapid than had been modeled (Fig. 5) indicating that our initial estimates of the mean heat capacity of these soils at or above field capacity was too high. From DOY 22 through 43, the controllers for belowground heating were reprogrammed and optimized. Full feedback control operating in an effective on–off protocol was in place from DOY 43 through 187. Self-optimizing procedures of the PID controller

Published 2010
This article is a US Government work and is in the public domain in the USA, *Global Change Biology*, doi: 10.1111/j.1365-2486.2010.02221.x

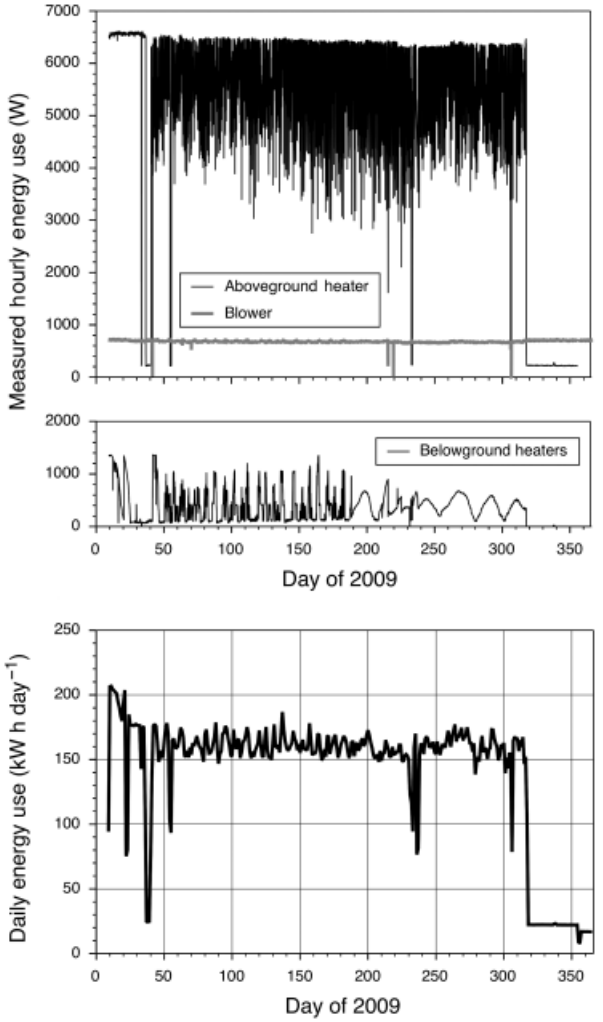

Fig. 4 Hourly energy needed to warm the air and belowground soils to −2 m in a 3 m diameter upland forest soil throughout 2009 (upper graph), and the daily cumulative total energy use for air and soil heating plus energy needed to operate blowers for air movement (lower graph).

were ineffective for three out of four of the heated belowground quadrants given the long feedback times. That is, the controllers continued to operate in an on–off mode through this time period. Manually optimized PID control was initiated on day 188 and run through the end of the warming period (DOY 317). Hourly energy use for both above- and belowground warming and associated equipment are provided in Fig. 4.

Air warming followed established experimental protocols of Norby *et al*. (1997) and immediately achieved the target differential air temperature during periods of low external atmospheric turbulence (recorded temperature data not shown). Under high wind conditions, the air warming capacity was periodically found to be inadequate to sustain the +4 °C mean air temperature differential. Variation in the energy demand for air heating through time is shown in Fig. 4. Air heaters with greater energy input capacities would be capable of achieving greater target air temperature differentials, but would still show variation in control capabilities with variable external winds.

Recorded mean soil temperatures from the surface to −200 cm are presented in Figs 5–7. Figure 5 demonstrates that target soil differentials between heated and control plots of +4 °C were achieved after DOY 59 when initial optimization of controls was accomplished. Differentials were subsequently maintained until DOY 317 when the power additions were stopped. Throughout the year, seasonal temperatures ranging from 0 to 25 °C and substantial rainfall inputs had little impact on the capacity of the experimental system to achieve target temperatures (Fig. 5). Drying of the top 30 cm of soil in the heated plots (Fig. 5, lower graph), which affects heat conduction of the soil volume had little impact on the ability of the method to achieve soil heating of +4 °C. The logic for feedback temperature control of the entire soil volume used simple comparative controls of air temperature at 1 m and soil temperatures at −0.76 m. That specific depth (C-80 in Fig. 5, upper graph) came closest to sustaining the target differential of +4 °C. Rainfall events indicated by the oscillating pattern of soil water content in Fig. 5 (lower graph) did have a small influence on the temperature treatments as either cooler or warmer water percolated through the soil profile.

Figure 6 shows measured mean hourly soil temperatures for all soil depths in the heated and control plots throughout the equilibrium-heating period. Following establishment of enhanced deep soil temperature elevation (i.e., by DOY 50; see also Fig. 5), data from Fig. 6 demonstrate that differentials were achieved throughout a full seasonal temperature cycle at all measured soil depths. Figure 7 shows the frequency distribution of hourly temperature occurrences for −5, −40 and −200 cm soil depths, contrasting the heated and control plots. Data are summarized for a 'wet' early season period (DOY 60–140; Fig. 7, upper graphs) and a mid-season dry period (DOY 190–270; Fig. 7, lower graphs). The frequency diagrams emphasize that the new deep heating method provides enhanced warming over time and depth without inducing substantial changes in the short-term temperature dynamics of the soils. That is, the deep heating method allowed natural temperature dynamics to be retained, while inducing defined temperature differentials.

Consistent with the original energy balance simulations (Fig. 2), there was little horizontal spatial temperature variation within the interior of the plot. Near the plot edge, in the vicinity of the belowground heating

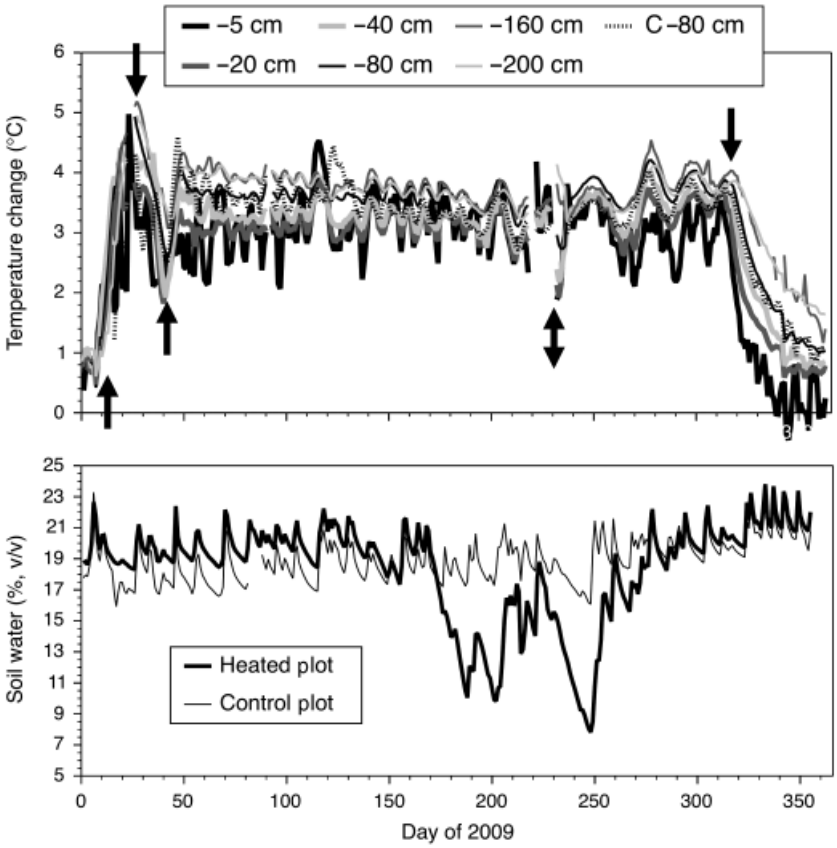

Fig. 5 Upper graph: Temperature differentials at multiple soil depths achieved following the initiation of treatments on January 7, 2009. The depth indicated as C-80 cm is the actual control depth. Data at other depths were obtained from independent thermocouple arrays located in the center and at mid-radius locations of the 3 m diameter circular plot. Lower graph: Measured surface soil water content data (0 to −30 cm) for the heated and control plots. Arrows in upper graph indicate transitions for power addition or removal to the belowground system.

elements, we also found little variation in mean soil temperatures at 50 or 20 cm from the heaters, and minimal temperature gradients between heaters at those distances (data not shown). Finally, although this heating method produced a rapid rise of soil temperatures in January (15 days), cooling of the soil horizons to near-ambient conditions following the removal of active heating on DOY 317 occurred at a slower pace requiring from 20 to 40 days to approach preheating levels dependent on the soil depth.

Heating influences on atmospheric humidity

During mid-summer periods with air temperatures of the heated plot ranging from 24 to 25 °C, and before steam injections were initiated, measured relative humidity of air (Fig. 8, top graph) averaged 20.2% units lower than values measured in the control plots (Fig. 8, middle graph). Vapor pressure deficits between surface soil water and air were also elevated (Fig. 8, lower graph). In an attempt to demonstrate that such humidity differentials could be controlled, steam additions were initiated mid-season (DOY 222) using a steam injection system capable of adding water vapor into the heated airflow at a rate of 6.2 kg H_2O h^{-1}. Figure 8 (middle graph) demonstrates the effectiveness of this method to add humidity and drop measured humidity differences from 20 to approximately 10%. Unfortunately, the largest steam injector that could be operated on the available single-phase power supply did not have sufficient capacity to completely overcome the differential vapor pressure gradients imposed by the air heating approach. Systems to provide the necessary water vapor injections would be available if sufficient power and water supplies were locally available. It is worth noting that the energy required to eliminate only half of the observed relative humidity difference was 84 kW h day^{-1} for the 3 m diameter chamber operating at three air exchanges per minute. That energy use rate for steam injection was 60% of the energy required to warm the air itself. A system adequate to remove the humidity differentials between heated and control plots

Published 2010
This article is a US Government work and is in the public domain in the USA, *Global Change Biology*, doi: 10.1111/j.1365-2486.2010.02221.x

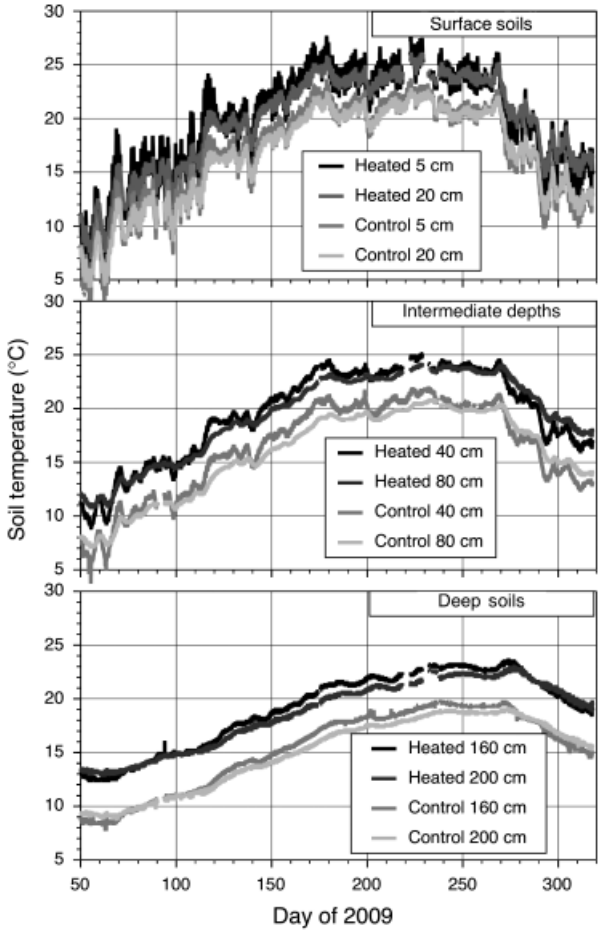

Fig. 6 Measured soil temperatures of heated and control plots by soil depth. Upper, middle and lower graphs include data for surface, intermediate and deep soil depths.

would likely demand as much or more energy than that required to warm the air itself unless air exchange volumes could be reduced.

Biological response

To illustrate the biological importance of this new deep soil warming technology, automated data for soil CO_2 efflux from the forest floor is provided in Fig. 9. Elevated soil temperatures from the surface to −200 cm were correlated with an instantaneous increase in CO_2 efflux from the forest floor, which was then sustained throughout the active warming period (DOY 7–317; Fig. 9). This increased efflux was not expressed as enhanced efflux along a defined temperature response curve, but an overall elevation to a response curve above the response data observed for the control plot soils (Fig. 9, right graph).

Discussion

Prior experiments for warming *in situ* field plots or intact peat monoliths used various methods for directly or indirectly warming the air, vegetation and soils with differing degrees of success. The main limitation of previous methods has been poor or inadequately characterized performance of soil heating at depth. The belowground heating method reported here removes this limitation.

Air and surface warming methods

An *in situ* method based on passive heat retention by greenhouse structures (Hollister *et al.*, 2006) achieved soil warming from near zero to 2 °C in the treated zone down to −30 cm in Alaska with attenuation of the warming capacity at −45 cm in dry heath. Passive warming greenhouses are dependent on near-term radiation regimes to provide differential warming treatments; during the night and extended dark winter periods they become incapable of sustaining the warming treatments. Kennedy (1995) concluded that passive greenhouses in Antarctica achieved only a 'poor simulation of GCM forecasts.'

Air warming and surface infrared warming can effectively warm surface soils, but the level of warming is attenuated by depth and is reduced with highly turbulent atmospheric conditions. In alpine tundra, Harte *et al.* (1995) showed that infrared warming set up for constant heat additions produced soil warming consistently in the range of +0.5 to +1.5 °C as deep as −25 cm, but found that the effectiveness of the technique was not consistent throughout a seasonal exposure period. Within isolated and horizontally insulated bog and fen mesocosms, Bridgham *et al.* (1999) attained 1.6–4.1 °C peat warming to depths of −40 cm, but the levels of differential warming were dependent on external environmental conditions and season of the year. Nijs *et al.* (2000) showed that surface soil warming was attenuated from 3 to 2 °C with depths to −20 cm in tundra. Kimball (2005) developed the energy balance theory necessary to plan and project the performance of infrared heaters and arrays for warming short vegetation canopies and tested the theory in grasslands (Kimball *et al.*, 2007). They demonstrated a clear capability to control vegetation canopy temperatures and soil temperatures at −10 cm, but provided no data on soil temperatures at greater depths. Enhancements of the Norby *et al.* (1997) air warming system to include an insulated block of soil to a depth of 0.75 m beneath a 4 m diameter chamber with air heated to +3.0 °C (Wan *et al.*, 2007) improved soil warming beneath their air heated chambers. During 2007, the difference in air temperature between warmed and ambient tempera-

This article is a US Government work and is in the public domain in the USA, *Global Change Biology*, doi: 10.1111/j.1365-2486.2010.02221.x

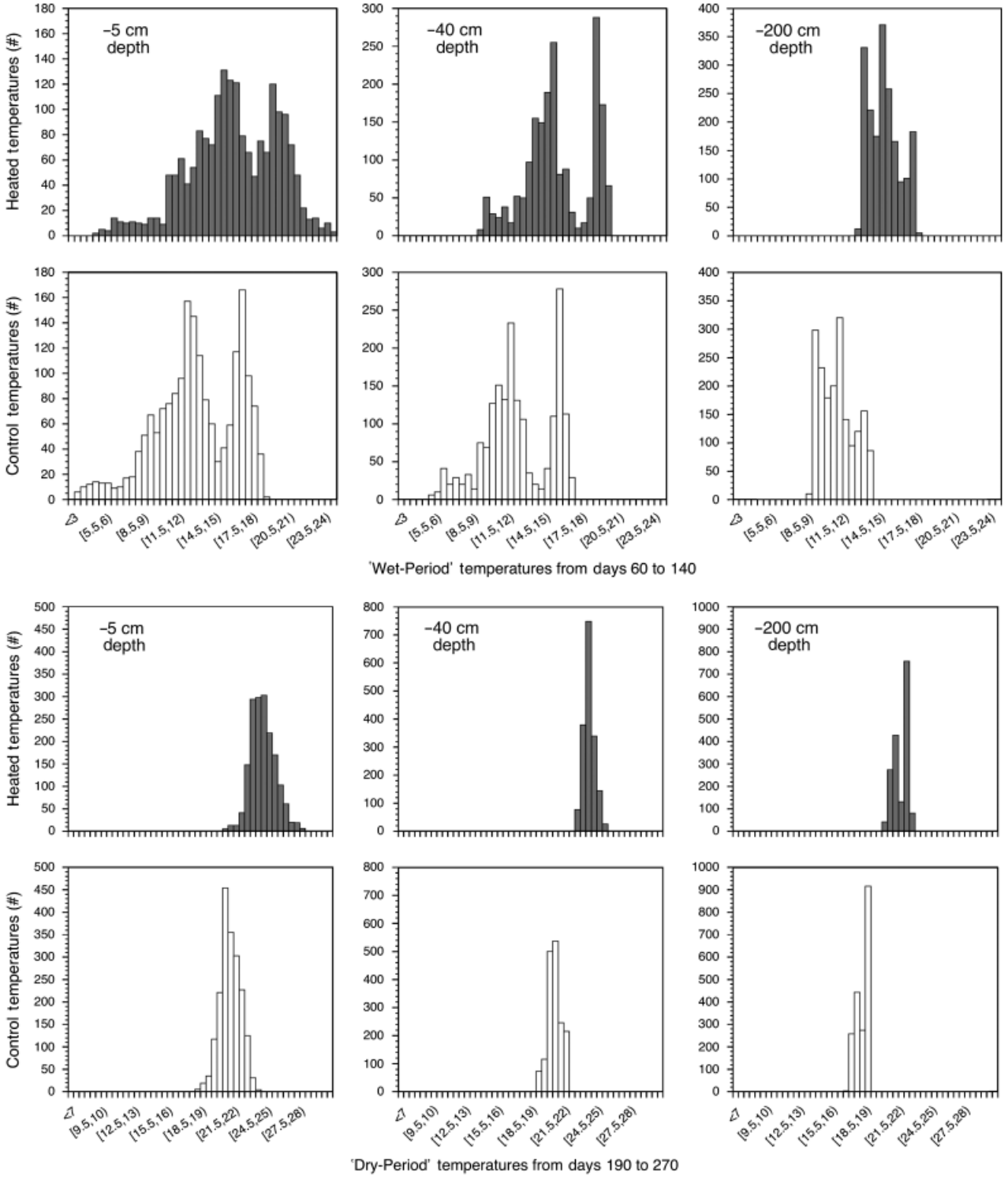

Fig. 7 Frequency distributions of temperature occurrences for the binned temperature ranges (x-axes) for high soil moisture conditions from DOY 60 to 140 (upper graphs), and a dry period from DOY 190 to 270 (lower graphs). Within the wet and dry groupings, occurrences of temperatures are plotted for both heated and control plots for −5, −40 and −200 cm soil depths.

Published 2010
This article is a US Government work and is in the public domain in the USA, *Global Change Biology*, doi: 10.1111/j.1365-2486.2010.02221.x

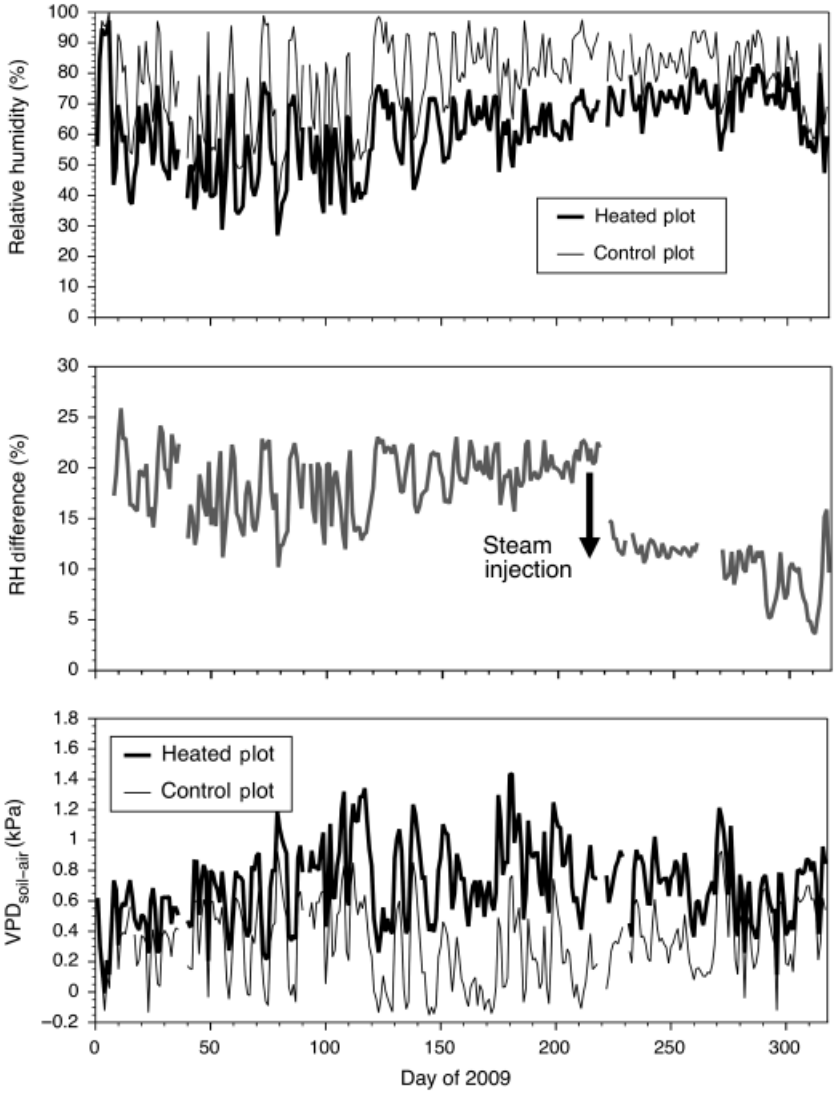

Fig. 8 Seasonal patterns of relative humidity (RH; upper graph), the difference between RH of the heated and control plot (middle graph), and the observed vapor pressure deficit (VPD) from surface soil moisture to free air (lower graph) measured throughout 2009. Steam injections at approximately 6.2 kg water vapor per hour were initiated into the heated plot on day 222 (see arrow middle graph).

ture chambers averaged 3.0 °C, and the soil temperature differential was 1.6–1.9 °C from 0 to 30 cm depth, but there are no data from deeper soil (R. Norby, unpublished results; http://warming.ornl.gov/OCCAM/data.html). The new air and deep soil heating method described here does not have the depth or temperature differential limitations of earlier studies, and can reproduce consistent temperature treatments corresponding to future warming scenarios.

Soil warming methods

Direct soil warming with buried cables (5–30 cm) has been shown to provide deeper effective warming into the soil profile (NSF, 1991; Peterjohn *et al.*, 1993), but such methods include substantial disturbance effects and localized horizontal thermal gradients within a biologically active portion of the soil profile. Peterjohn *et al.*, (1994) used heating cables buried beneath the humus layer in Massachusetts to achieve +5 °C soil temperature warming in the surface soils. Rustad & Fernandez (1998) similarly used buried cables 1–2 cm below the O-horizon in a Maine forest and reported mean warming from May through November of approximately +4 °C at −10 cm attenuated to +3 °C at −50 cm. Ineson *et al.* (1998) deployed a mesh surface heating method for use under grass canopies that showed rapid deterioration of the soil heating with

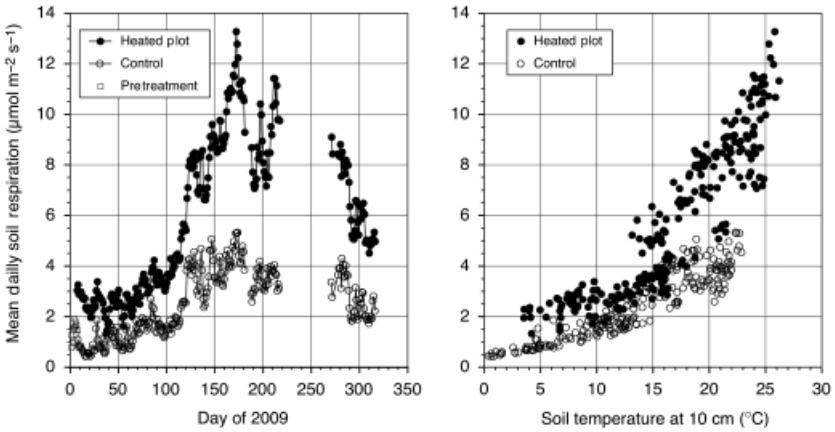

Fig. 9 The response of soil respiration to the heating treatments of the newly designed warming plots.

depth from around +3 °C in the top 5 cm to only +1 °C at −30 cm. Strömgren & Linder (2002), also using the approach of Peterjohn *et al*. (1994), reported warming of surface soils in the range of +4 to +6 °C that extended to similar warming at −50 cm. Direct soil heating methods can and have produced soil temperature profiles that were consistent with climatic warming scenarios. Bronson *et al*. (2008, 2009) combined aboveground air warming with heating cables buried at −20 cm and were able to maintain consistent air and soil surface warming at −10 cm near their target temperature differential of +5 °C through three growing seasons. Although Bronson *et al*. (2008) indicate that they measured soil temperatures as deep as −100 cm, the effectiveness of their warming method at such depths was not published. The deep circumferential method for soil warming described in this paper extends soil warming to even deeper soils and avoids the pitfall of direct installation disturbance in biologically active soil profiles.

Performance issues for deep soil heating

Air and soil heating treatments led to significant drying of the surface soils and litter layer of the experimental plots (Fig. 7 and unpublished litter-layer moisture data). Latent energy transfer associated with surface drying consumed local heat energy and reduced temperature differentials recorded at −5 and −20 cm. With the addition of partial humidification on DOY 222 latent energy consumption by evaporation would have been reduced and temperature differentials increased towards the target of a full +4 °C differential. A clear demonstration that surface drying acts as an energy sink to limit attainment of surface soil temperature differentials in shallow soils remains to be demonstrated in theoretical models or with the installation of sufficient steam capacities to eliminate the heating-induced enhancement of vapor pressure deficits from soil to air (Fig. 8).

Belowground heating using the method described here uses a very gradual addition of thermal energy to achieve target soil temperature differentials. Belowground heater casing surface temperatures were never >27 °C throughout the year and therefore did not expose soil to extreme temperature conditions that might impact soil biological, chemical or physical characteristics or pose a danger for fire ignition. Variable water content was also not an impediment to successful belowground warming. For mineral soils with water contents ranging from wet to dry conditions (Fig. 5, lower graph), this method of energy addition was able to sustain +4 °C soil temperature differentials. Simulated heat transfer values for water, mineral matter and rocks plus organic matter suggest that the deep soil warming approach should have broad applicability across ecosystems.

Shaver *et al*. (2000) and Aronson & McNulty (2009) both summarized a variety of experimental methods used to evaluate biological responses of plants and microorganisms to warming. Both groups concluded that all methods have value and can be used to identify mechanistic responses at one or more spatiotemporal scales. In this paper, we add an additional technology to the warming experimental arsenal. Using control points for air temperature at 1 m and for soil temperatures at a fixed deep location we demonstrate a capacity to control soil temperature differentials from the vegetated air space to deep positions within the soil profiles (Fig. 6). Although only demonstrated for a single target temperature differential in this paper, the method should be capable of direct continuous control of above- and belowground temperature differentials at specified levels consistent with a wide range of climate change projections.

Published 2010
This article is a US Government work and is in the public domain in the USA, *Global Change Biology*, doi: 10.1111/j.1365-2486.2010.02221.x

Importance of deep heating to soil biology

Surface soil efflux (often termed soil respiration) is the complex combination of root, mycorrhizal fungi and heterotrophic microbial activities (fungi and bacteria) belowground. Enhanced soil CO_2 efflux from the ground is a dominant, but not universal response to warming manipulations (Rustad & Fernandez, 1998; Rustad *et al*., 2001; Oberbauer *et al*., 2007; Bronson *et al*., 2008).

We had anticipated that soil warming would result in a proportionate increase consistent with the ambient temperature response curve (Fig. 9, left box), but we found a disproportionate increase in soil CO_2 efflux above the data for control conditions. We believe these data demonstrate that deep belowground treatment systems produce enhanced biological activity in a manner never before measured under manipulated field-experiment conditions.

Oberbauer *et al*. (2007) showed variable levels of enhanced ecosystem respiration (including aboveground plant respiration) within passive hexagonal open top chambers for arctic sites of North America. In that study, warming enhanced surface CO_2 efflux, but responses remained on a single temperature response curve. Warming induced increases in soil CO_2 efflux reported by Peterjohn *et al*. (1994) also followed a single temperature response curve with heated plot respiration rates simply being pushed outward along a nearly identical temperature response curve. Soil CO_2 efflux temperature relationships reported by Bronson *et al*. (2008) were either consistent with the general form of their control plot response curves or they fell below them. They attributed changes to potential changes in root density with depth. Melillo *et al*. (2002) report sustained observations of soil respiration with direct soil warming over multiple growing seasons, and concluded that initial strong responses to direct soil heating were attenuated over time due to reductions in labile carbon stocks within the warmed soil profile.

Future applications of the deep soil heating method over longer time periods will need to be combined with depth-specific measures of root mass density, root respiration activity, labile carbon pool availability, and the activity of soil microbial populations to clarify the complex nature of heating-induced changes in soil CO_2 efflux. Nevertheless, the success of deep heating reported here, along with the measured and unexpectedly high enhancement of soil CO_2 efflux, suggest the potentially important application of a deep soil warming technology to capture appropriate responses of ecological systems to future warming scenarios. This may be especially true in high-carbon fens, ombrotrophic bogs and in permafrost regions where experimental deep soil warming consistent with future climate projects has yet to be achieved (Shaver *et al*., 2000).

Energy needs for routine operation

Energy use for heating both the above- and belowground warming components of the 3 m prototype to $+4\,^{\circ}C$ were assessed for equilibrium maintenance of the temperature differentials from February 28, 2009 through November 12, 2009. This measurement period excludes the warm-up and debugging period of operation of the prototype that began on January 7, 2009. It does include soil water contents at field capacity or above (during rain events), dry summer periods (Fig. 5), and a rewetting period throughout the autumn of 2009. The mean daily rate of energy use for the 3 m prototype with an effective heated ground area of 7.1 m^2 included belowground heating at 9.1 $kW\,h\,day^{-1}$ or 1.3 $kW\,h\,day^{-1}\,m^{-2}$, and aboveground heating at 150.0 $kW\,h\,day^{-1}$ or 21.1 $kW\,h\,day^{-1}\,m^{-2}$. This energy expenditure of approximately 4700 kW h per month is equivalent to that used to cool a very large home during the hot summer months. The current prototype has an air turnover rate of 3.3 times per minute. That level of air turnover may not be essential or desirable to the warming treatments or to the elevation of CO_2 in future studies. Heating requirements calculated on an air turnover rate of only one exchange per minute would be 0.39 $kW\,h\,day^{-1}\,m^{-2}$ for belowground heating and 6.39 $kW\,h\,day^{-1}\,m^{-2}$ for aboveground heating.

The levels of energy input are significant. At \$0.10 $kW\text{-}h^{-1}$ direct scaling of the measured energy use for the 3 m prototype (7.1 m^2 of treated ground area) to, for example, the scale of 20 m diameter free air CO_2 treatment plot area (314 m^2 treated ground area) would lead to daily operational costs of approximately \$2000 day^{-1} (\$120 for belowground heating). That cost does not include the expense of constructing and maintaining appropriately sized, aboveground, transparent walls for analogy to this application.

Warming at ecosystem-relevant scales clearly remains a daunting and expensive challenge. New aboveground warming methods combined with the belowground concept described in this paper should nevertheless be conceived for appropriately scaled ecosystems to facilitate manipulative experiments appropriate to future climate conditions.

Conclusions

This paper describes a combination of air warming and new methods for inducing deep-soil warming capable of sustaining target differential temperatures through-

This article is a US Government work and is in the public domain in the USA, *Global Change Biology*, doi: 10.1111/j.1365-2486.2010.02221.x

out the soil profile (soil surface to −200 cm). The method worked throughout an annual cycle of temperatures, precipitation events and soil moisture conditions in an upland oak forest of eastern Tennessee. Both diel variations and seasonal temperature dynamics of the ambient environment were conserved. Additional simulations (not discussed here) suggested that the method could be applied to larger spatial areas, and the physical principals should be applicable to a wide range of soil conditions. The method may also be appropriate for application with aboveground infrared heating methods on short vegetation.

The method is indeed energy intensive to operate, but the energy demands for enabling belowground warming in a climatically appropriate manner represent a fraction of the total energy requirements for whole-ecosystem warming. Unexpected enhancement of soil CO_2 efflux from these deep warming treatments suggests that past warming studies without effective deep warming may have underestimated the responsiveness of soil biological communities to future warming. Technologies that enable the application of deep soil warming should be considered and applied to experiments designed to understand the impacts of climatic change.

Acknowledgements

Development of the belowground warming method was accomplished with support from the Laboratory Directed Research and Development program at Oak Ridge National Laboratory. Additional support following internal development was provided by the U.S. Department of Energy (DOE), Office of Science, Biological and Environmental Research. Oak Ridge National Laboratory (ORNL) is managed by UT-Battelle, LLC, for the DOE under contract DE-AC05-00OR22725.

References

Amthor JS, Hanson PJ, Norby RJ, Wullschleger SD (2010) A comment on ''Appropriate experimental ecosystem warming methods by ecosystem, objective, and practicality'' by Aronson and McNulty''. *Agricultural and Forest Meteorology*, **150**, 497–498.

Aronson EL, McNulty SG (2009) Appropriate experimental ecosystem warming methods by ecosystem, objective, and practicality. *Agricultural and Forest Meteorology*, **149**, 1791–1799.

Baxter DO (1997) A comparison of deep soil temperature: Tennessee versus other locations. *Transactions of the ASAE*, **40**, 727–738.

Bridgham SD, Pastor J, Updegraff K, Malterer TJ, Johnson K, Harth C, Chen J (1999) Ecosystem control over temperature and energy flux in northern peatlands. *Ecological Applications*, **9**, 1345–1358.

Bronson DR, Gower ST, Tanner M, Van Herk I (2009) Effect of ecosystem warming on boreal black spruce bud burst and shoot growth. *Global Change Biology*, **15**, 1534–1543.

Bronson DR, Gower ST, Tanner M, Linder S, Van Herk I (2008) Response of soil surface CO_2 flux in a boreal forest to ecosystem warming. *Global Change Biology*, **14**, 856–867.

Childs KW (1993) *Heating 7.2 User's Manual, ORNL/TM-12262*. Oak Ridge National Laboratory, Oak Ridge, TN, USA.

Christensen JH, Hewitson B, Busuioc A *et al*. (2007) Regional climate projections. In: *Climate Change 2007: The Physical Science Basis. Contribution of Working Group I to the Fourth Assessment Report of the Intergovernmental Panel on Climate Change* (eds Solomon S, Qin D, Manning M, Chen Z, Marquis M, Averyt KB, Tignor M, Miller HL), pp. 847–940. Cambridge University Press, Cambridge, UK.

Dermody O, Weltzin JF, Engel EC, Allen P, Norby RJ (2007) How do elevated [CO_2], warming, and reduced precipitation interact to affect soil moisture and LAI in an old field ecosystem? *Plant and Soil*, **301**, 255–266.

Gunderson CA, O'hara KH, Campion CM, Walker AV, Edwards NT (2010) Thermal plasticity of photosynthesis: the role of acclimation in forest responses to a warming climate. *Global Change Biology*, (in press), doi: 10.1111/j.1365-2486.2009.02090.x

Hanson PJ, Classen A, Kueppers LWorkshop Participants (2008) *Ecosystem experiments: understanding climate change impacts on ecosystems and feedbacks to the physical climate*. Report of the workshop on Exploring Science Needs for the Next Generation of Climate Change and Elevated-CO_2 Experiments in Terrestrial Ecosystems, April 14–18, 2008, Arlington, VA (white paper report submitted to DOE).

Hanson PJ, O'Neill EG, Chambers MLS, Riggs JS, Joslin JD, Wolfe MH (2003) Soil respiration and litter decomposition. In: *North American Temperate Deciduous Forest Responses to Changing Precipitation Regimes. Ecological Studies*, Vol. 166. (eds Hanson PJ, Wullschleger SD), pp. 163–189. Springer, New York.

Hanson PJ, Wullschleger SD, eds (2003) *North American Temperate Deciduous Forest Responses to Changing Precipitation Regimes. Ecological Studies*, Vol. 166. Springer, New York.

Harte J, Torn MS, Chang F-R, Feifarek B, Kinzig AP, Shaw R, Shen K (1995) Global warming and soil microclimate: results from a meadow-warming experiment. *Ecological Applications*, **5**, 132–150.

Hegerl GC, Crowley TJ, Allen M, Hyde WT, Pollack HN, Smerdon J, Zorita E (2007) Detection of human influence on a new, validated 1500-year temperature reconstruction. *Journal of Climate*, **20**, 650–666.

Hollister RD, Webber PJ, Nelson FE, Tweedie CE (2006) Soil thaw and temperature response to air warming varies by plant community: results from and open-top chamber experiment in northern Alaska. *Arctic, Antarctic, and Alpine Research*, **38**, 206–215.

Huang S (2006) Land warming as part of global warming. *EOS*, **87**, 477, 480.

Hu Q, Feng S (2003) A daily soil temperature dataset and soil temperature climatology of the contiguous United States. *Journal of Applied Meteorology*, **42**, 1139–1156.

Ineson P, Benham DG, Poskitt J, Harrison AF, Taylor K, Woods C (1998) Effects of climate change on nitrogen dynamics in upland soils. 2. A soil warming study. *Global Change Biology*, **4**, 153–161.

IPCC (2007) Alley RB and others, *Intergovernmental Panel on Climate Change (IPCC) Summary for Policymakers*. Contribution of Working Group I to the Fourth Assessment Report of the Intergovernmental Panel on Climate Change. Available at: http://ipcc-wg1.ucar.edu/wg1/wg1-report.html

Janzen HH (2009) Long-term ecological sites: musings on the future, as seen (dimly) from the past. *Global Change Biology*, **15**, 2770–2778.

Johnson DW, VanHook RI), eds (1989) *Analysis of Biogeochemical Cycling Processes in Walker Branch Watershed*. Springer-Verlag, New York.

Kennedy AD (1995) Temperature effects of passive greenhouse apparatus in high-latitude climate change experiments. *Functional Ecology*, **9**, 340–350.

Kimball BA (2005) Theory and performance of an infrared heater for ecosystem warming. *Global Change Biology*, **11**, 2041–2056.

Kimball BA, Conley MM, Wang S, Lin X, Luo C, Morgan J, Smith D (2007) Infrared heater arrays for warming ecosystem field plots. *Global Change Biology*, **14**, 309–320.

Medhurst J, Parsby J, Linder S, Wallin G, Ceschia E, Slaney M (2006) A whole-tree chamber system for examining tree-level physiological responses of field grown trees to environmental variation and climate change. *Plant, Cell and Environment*, **29**, 1853–1869.

Melillo JM, Steudler PA, Aber JD *et al*. (2002) Soil warming and the carbon-cycle feedbacks to the climate system. *Science*, **298**, 2173–2176.

Nijs I, Kockelbergh F, Heuer M, Beyens L, Tappeniers K, Impens I (2000) Climate-warming simulation in tundra: enhanced precision and repeatability with an improved infrared heating device. *Arctic, Antarctic, and Alpine Research*, **32**, 346–350.

Nijs I, Kockelbergh F, Teughels H, Blum H, Hendrey G, Impens I (1996) Free air temperature increase (FATI): a new tool to study global warming effects on plants in the field. *Plant, Cell and Environment*, **19**, 495–502.

NSF – National Science Foundation (1991) *Soil warming experiments in global change research*. The Report of a workshop held in Woods Hole, MA, September 27–28, 1991, (see p. 13).

Norby RJ, Edwards NT, Riggs JS, Abner CH, Wullschleger SD, Gunderson CA (1997) Temperature-controlled open-top chambers for global change research. *Global Change Biology*, **3**, 259–267.

Oberbauer SF, Tweedie CE, Welker JM *et al*. (2007) Tundra CO_2 fluxes in response to experimental warming across latitudinal and moisture gradients. *Ecological Monographs*, **77**, 221–238.

Peterjohn WT, Melillo JM, Bowles FP, Steudler PA (1993) Soil warming and trace gas fluxes: experimental design and preliminary flux results. *Oecologia*, **93**, 18–24.

Peterjohn WT, Melillo JM, Steudler PA, Newkirk KM, Bowles FP, Aber JD (1994) Responses of trace gas fluxes and N availability to experimentally elevated soil temperatures. *Ecological Applications*, **4**, 617–625.

Raupach MR, Marland G, Ciais P, Le Queré C, Canadell JG, Klepper G, Field CB (2007) Global and regional drivers of accelerating CO_2 emissions. *Proceedings of the National Academy of Sciences of the United States of America*, **104**, 10288–10293.

Rustad LE, Campbell JL, Marion GM *et al*. (2001) A meta-analysis of the response of soil respiration, net nitrogen mineralization, and aboveground plant growth to experimental ecosystem warming. *Oecologia*, **126**, 543–562.

Rustad LE, Fernandez IJ (1998) Experimental soil warming effects on CO_2 and CH_4 flux from a low elevation spruce-fir forest soil in Maine, USA. *Global Change Biology*, **4**, 597–605.

Shaver GR, Canadell J, Chapin FS III (2000) Global warming and terrestrial ecosystems: a conceptual framework for analysis. *Bioscience*, **50**, 871–882.

Strömgren M, Linder S (2002) Effects of nutrition and soil warming on stemwood production in a boreal Norway spruce stand. *Global Change Biology*, **8**, 1195–1204.

Tjoelker MG, Zhou X (2007) The many faces of climate warming. *New Phytologist*, **176**, 739–742.

Verburg PSJ, Larsen J, Johnson DW, Schorran DE, Arnone JA III (2005) Impacts of an anomalously warm year on soil CO_2 efflux in experimentally manipulated tallgrass prairie ecosystems. *Global Change Biology*, **11**, 1720–1732.

Wan S, Norby RJ, Ledford J, Weltzin JF (2007) Responses of soil respiration to elevated CO_2, air warming, and changing soil water availability in an old-field grassland. *Global Change Biology*, **13**, 2411–2424.

Published 2010
This article is a US Government work and is in the public domain in the USA, *Global Change Biology*, doi: 10.1111/j.1365-2486.2010.02221.x